Supporting Information

Dual-Modal Photon Upconverting and Downshifting Emissions from Ultra-Stable $CsPbBr_3$ Perovskite Nanocrystals Triggered by Co-Growth of Tm: $NaYbF_4$ Nanocrystals in Glass

Xiaoyan Li [a,b,c,d], Changbin Yang [a], Yunlong Yu [b,c], Zheng Li [a], Jidong Lin [a], Xiangfeng Guan [b], Zhiqiang Zheng [a, d, *], Daqin Chen [a, d, e, *]

[a] College of Physics and Energy, Fujian Normal University, Fuzhou 350117, China
E-mail: zqzheng@fjnu.edu.cn (Z. Q. Zheng); dqchen@fjnu.edu.cn (D. Q. Chen)

[b] College of Electronics and Information Science, Fujian Jiangxia University, Fuzhou 350108, China

[c] Key Laboratory of Green Perovskites Application of Fujian Province Universities, Fujian Jiangxia University, Fuzhou 350108, China

[d] Fujian Provincial Collaborative Innovation Center for Advanced High-Field Superconducting Materials and Engineering, Fuzhou 350117, China

[e] Fujian Provincial Engineering Technology Research Center of Solar Energy Conversion and Energy Storage, Fuzhou 350117, China

Table S1. Norminal glass compositions (mol%) for preparing dual-phase glasses containing Tm: $NaYbF_4$ UCNCs and $CsPbBr_3$ PQDs. The total mole content of glass composition is not fixed to 100% for better comparison throughout the text.

Composition (mol%)		GeO_2	B_2O_3	ZnO	CaO	Na_2O	PbO	CsBr	YbF_3	TmF_3
Sample	**S0**	50	20	5	3	6	0	12	5	0.1
	S1	50	20	5	3	6	1	12	5	0.1
	S2	50	20	5	3	6	3	12	5	0.1
	S3	50	20	5	3	6	5	12	5	0.1
	S4	50	20	5	3	6	7	12	5	0.1
	S5	50	20	5	3	6	3	8	5	0.1
	S6	50	20	5	3	6	3	16	5	0.1
	S7	50	20	5	3	6	3	20	5	0.1
	S8	50	20	5	3	6	3	12	3	0.1
	S9	50	20	5	3	6	0	12	8	0.1
	S10	50	20	5	3	6	1	12	8	0.1
	S11	50	20	5	3	6	3	12	8	0.1
	S12	50	20	5	3	6	5	12	8	0.1
	S13	50	20	5	3	6	7	12	8	0.1
	S14	50	20	5	3	6	3	8	8	0.1
	S15	50	20	5	3	6	3	16	8	0.1
	S16	50	20	5	3	6	3	20	8	0.1

The mole contents of PbO (x mol%, x=1, 3, 5, 7), CsBr (y mol%, y=8, 12, 16, 20) and YbF_3 (z mol%, z=3, 5, 8) components in the glasses are modified to achieve dual-phase glasses with desirable crystallization phases and optimal optical performance.

Table S2. The fitted decay parameters for PL and UC exciton recombination of $CsPbBr_3$ PQDs in dual-phase glasses with different PbO contents (x=1, 3, 5, 7 mol%, fixed 12 mol% CsBr, 5 mol% YbF_3).

		A_1	τ_1 (ns)	A_2	τ_2 (ns)	A_3	τ_3 (ns)	τ_{ave} (ns)
PL	x=1	3752	9.67	1622	50.11	258	258.82	117
PL	x=3	5390	12.11	2523	62.95	479	286.72	138
PL	x=5	4357	5.40	1284	36.24	140	186.56	69
PL	x=7	4540	4.32	1044	24.65	129	114.26	40
		A_1	τ_1 (μs)	A_2	τ_2 (μs)	A_3	τ_3 (μs)	τ_{ave} (μs)
UC	x=3	9461	185.00	1446	351.09	--	--	222

Owing to their non-single-exponential features, PL decay curves of exciton recombination can be described by the following three-exponential expression

$$I = A_1 exp\left(-\frac{t}{\tau_1}\right) + A_2 exp\left(-\frac{t}{\tau_2}\right) + A_3 exp\left(-\frac{t}{\tau_3}\right)$$

Where A_1, A_2 and A_3 are the fitting constants, τ_1, τ_2 and τ_3 are the corresponding decay times, respectively. The average lifetime can be determined by the following equation

$$\tau_{ave} = (A_1\tau_1^2 + A_2\tau_2^2 + A_3\tau_3^2)/(A_1\tau_1 + A_2\tau_2 + A_3\tau_3)$$

All the values are tabulated in **Table S2**.

Similarly, UC decay curves of exciton recombination can be described by the two-exponential expression and the related parameters are also provided in **Table S2** for comparison.

Derivation of absolute temperature sensitivity and relative sensitivity

In the investiaged dual-phase embedded glass, exciton recombination and Tm^{3+} $^3F_{2,3}\rightarrow{}^3H_6$ transition are temperature detecting signals for their significant temperature-sensitive emissions, while Tm^{3+}: $^1G_4\rightarrow{}^3H_6$ and $^1G_4\rightarrow{}^3F_4$ transitions act as the reference signals for their relatively temperature-insensitive emissions. Herein, FIR1 can be easily deduced according to the expression of temperature-dependent exciton recombination [S1,S2]

$$FIR1 = \frac{I_{PQDs\ em}}{I_{477\ nm}} \approx \frac{1}{B + Cexp(^{-\Delta E}/_{k_B T})}$$

where B and C are constants, T is absolute temperature, k_B is Boltzmann constant. ΔE is nominal thermal quenching activation energy for the $CsPbBr_3$ PQDs and Tm^{3+} $^1G_4 \rightarrow {}^3H_6$ dual-emitting system. On the other hand, FIR2 data can be well fitted to temperature by the following exponential equation [S3,S4]

$$FIR2 = \frac{I_{707\ nm}}{I_{650\ nm}} = D + E \times exp(^{-F}/_{T})$$

where D, E and F are constants.

According to these two FIR equations, absolute temperature sensitivity (S_a) and relative temperature sensitivity (S_r) can be further derived and expressed by the following equations.

For FIR1

$$S_{a(523/477)} = \left|\frac{\partial FIR1}{\partial T}\right| = \frac{Cexp(^{-\Delta E}/_{k_B T})}{\left[B + Cexp(^{-\Delta E}/_{k_B T})\right]^2} \times \frac{\Delta E}{k_B T^2}$$

$$S_{r(523/477)} = \left|\frac{1}{FIR}\frac{\partial FIR1}{\partial T}\right| \times 100\% = \frac{Cexp(^{-\Delta E}/_{k_B T})}{B + Cexp(^{-\Delta E}/_{k_B T})} \times \frac{\Delta E}{k_B T^2} \times 100\%$$

For FIR2

$$S_{a(707/650)} = \left|\frac{\partial FIR2}{\partial T}\right| = exp(^{-F}/_{T}) \times \frac{EF}{T^2}$$

$$S_{r(707/650)} = \left|\frac{1}{FIR}\frac{\partial FIR2}{\partial T}\right| \times 100\% = \frac{exp(^{-F}/_{T})}{D + E \times exp(^{-F}/_{T})} \times \frac{EF}{T^2} \times 100\%$$

References

[S1] Li, X.; Wu, Y.; Zhang, S.; Cai, B.; Gu, Y.; Song, J.; Zeng, H. $CsPbX_3$ Quantum Dots for Lighting and Displays: Room-Temperature Synthesis, Photoluminescence Superiorities, Underlying Origins and White Light-Emitting Diodes. *Adv. Funct. Mater.* **2016**, *26*, 2435-2445.

[S2] Yuan, S.; Chen, D.; Li, X.; Zhong, J.; Xu, X. In Situ Crystallization Synthesis of $CsPbBr_3$ Perovskite Quantum Dot-Embedded Glasses with Improved Stability for Solid-State Lighting and Random Upconverted Lasing. *ACS Appl. Mater. Interfaces* **2018**, *10*, 18918-18926.

[S3] Chen, D.; Liu, S.; Wan, Z.; Chen, Y. A Highly Sensitive Upconverting Nano-Glass-Ceramic-Based Optical Thermometer. *J. Alloys Compd.* **2016**, *672*, 380-385.

[S4] Xu, W.; Zhang, Z.; Cao, W. Excellent Optical Thermometry Based on Short-Wavelength Upconversion Emissions in Er^{3+}/Yb^{3+} Co-doped $CaWO_4$. *Opt. Lett.* **2012**, *37*, 4865.

Table S3. Absolute/relative sensitivities and temperature range of optical temperature sensors based on several typical luminescent materials.

Sensing materials	FIR	Temperature range (K)	Maximal S_a (K^{-1})	Maximal S_r (% K^{-1})	Ref.*
Tm^{3+}: YF_3 glass ceramic	$I_{(Tm^{3+}:{}^3F_{2,3}\rightarrow{}^3H_6)}$ / $I_{(Tm^{3+}:{}^1G_4\rightarrow{}^3F_4)}$	293-563	0.0184	--	[S3]
Tm^{3+}/Yb^{3+}: $Y_2Ti_2O_7$ phosphor	$I_{(Tm^{3+}:{}^3F_{2,3}\rightarrow{}^3H_6)}$ / $I_{(Tm^{3+}:{}^1G_4\rightarrow{}^3H_6)}$	293-398	--	0.81	[S5]
Tm^{3+}/Yb^{3+}: $SrWO_4$	$I_{(Tm^{3+}:{}^3F_3\rightarrow{}^3H_6)}$ / $I_{(Tm^{3+}:{}^3H_4\rightarrow{}^3H_6)}$	308-573	0.0062	--	[S6]
$Ho^{3+}/Tm^{3+}/Yb^{3+}$: $Ba_3Y_4O_9$	$I_{(Tm^{3+}:{}^3H_4\rightarrow{}^3H_6)}$ / $I_{(Tm^{3+}:{}^1G_4\rightarrow{}^3H_6)}$	293-473	0.0552	0.34	[S7]
Pr^{3+}: $LaMg_{0.402}Nb_{0.598}O_3$	$I_{(Pr^{3+}:{}^1D_2\rightarrow{}^3H_4)}$ / $I_{(Pr^{3+}\ {}^3P_0\rightarrow{}^3F_2)}$	298-523	0.0597	0.73	[S8]
CD/ RhB	I_{CD}/I_{RhB}	283-373	0.0201	1.39	[S9]
dual-phase glass	$I_{PQDs\ em}$ / $I_{(Tm^{3+}:{}^1G_4\rightarrow{}^3H_6)}$	77-350	0.0474	0.98	This work
dual-phase glass	$I_{(Tm^{3+}:{}^3F_{2,3}\rightarrow{}^3H_6)}$ / $I_{(Tm^{3+}:{}^1G_4\rightarrow{}^3F_4)}$	300-700	0.4381	1.35	This work

*References

[S5] Tu, X.; Xu, J.; Li, M.; Xie, T.; Lei, R.; Wang, H.; Xu, S. Color-Tunable Upconversion Luminescence and Temperature Sensing Behavior of Tm^{3+}/Yb^{3+} Codoped $Y_2Ti_2O_7$ Phosphors. *Mater. Res. Bull.* **2019**, *112*, 77-83.

[S6] Song, H.; Wang, C.; Han, Q.; Tang, X.; Yan, W.; Chen, Y.; Jiang, J.; Liu, T. Highly Sensitive Tm^{3+} /Yb^{3+} Codoped $SrWO_4$ for Optical Thermometry. *Sensor. Actuat. A Phys.* **2018**, *271*, 278-282.

[S7] Liu, S.; Cui, J.; Jia, J.; Fu, J.; You, W.; Zeng, Q.; Yang, Y.; Ye, X. High Sensitive $Ln^{3+}/Tm^{3+}/Yb^{3+}$ (Ln^{3+}= Ho^{3+}, Er^{3+}) Tri-Doped $Ba_3Y_4O_9$ Upconverting Optical Thermometric Materials Based on Diverse Thermal Response from Non-Thermally Coupled Energy Levels. *Ceram. Int.* **2019**, *45*, 1-10.

[S8] Zhang, H.; Gao, Z.; Li, G.; Zhu, Y.; Liu, S.; Li, K.; Liang, Y. A Ratiometric Optical Thermometer with Multi-Color Emission and High Sensitivity Based on Double Perovskite $LaMg_{0.402}Nb_{0.598}O_3$: Pr^{3+} Thermochromic Phosphors. *Chem. Eng. J.* **2020**, *380*, 122491.

[S9] Zhu, Z.; Sun, Z.; Guo, Z.; Zhang, X.; Wu, Z. chao. A High-Sensitive Ratiometric Luminescent Thermometer Based on Dual-Emission of Carbon Dots/Rhodamine B Nanocomposite. *J. Colloid Interface Sci.* **2019**, *552*, 572-582.

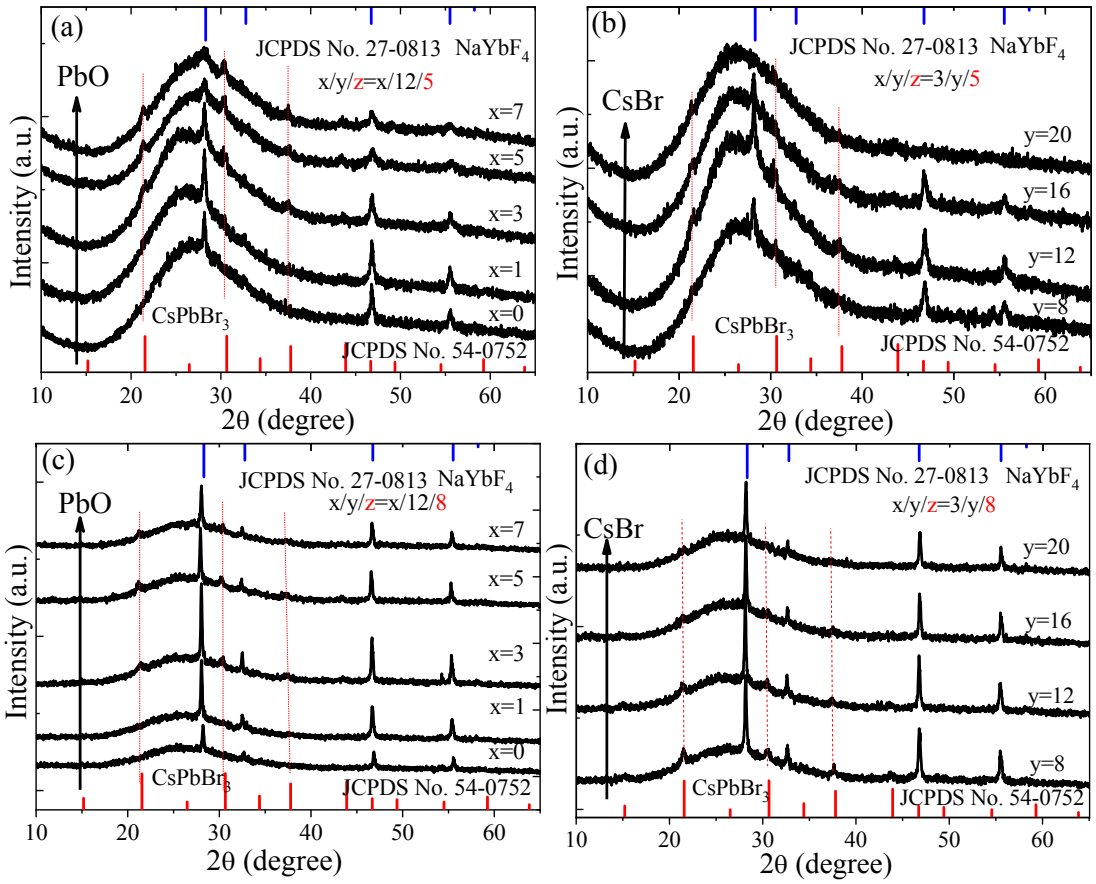

Figure S1. XRD patterns of a series of dual-phase glass samples: (a) different PbO contents (fixed 12 mol% CsBr and 5 mol% YbF_3), (b) different CsBr contents (fixed 3 mol% PbO and 5 mol% YbF_3), (c) different PbO contents (fixed 12 mol% CsBr and 8 mol% YbF_3) and (d) different CsBr contents (fixed 3 mol% PbO and 8 mol% YbF_3). Bars represent standard diffraction peaks of cubic $NaYbF_4$ (JCPDS No. 27-0813) and cubic $CsPbBr_3$ (JCPDS No. 54-0752) crystals.

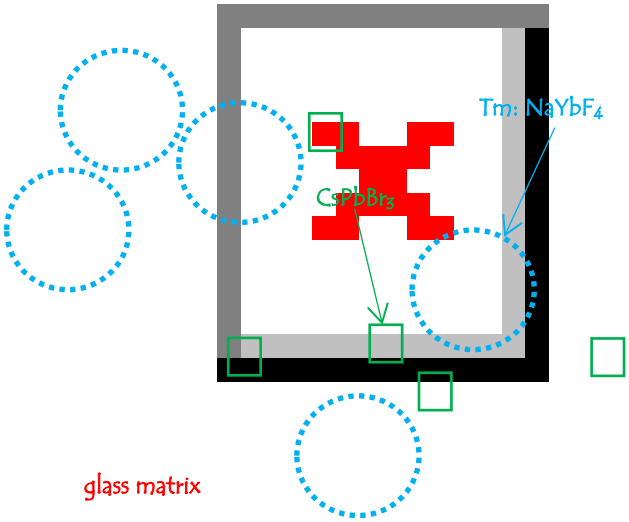

Figure S2. HAADF-STEM micrograph for a typical $CsPbBr_3$ and $NaYbF_4$ dual-phase embedded glass, showing the co-existence of small-size $CsPbBr_3$ PNCs (bright contrast) and large-size Tm: $NaYbF_4$ UCNCs (bright contrast) inside glass matrix (dark contrast). Some of $CsPbBr_3$ PNCs and Tm: $NaYbF_4$ UCNCs are marked by circle and rectangle, respectively.

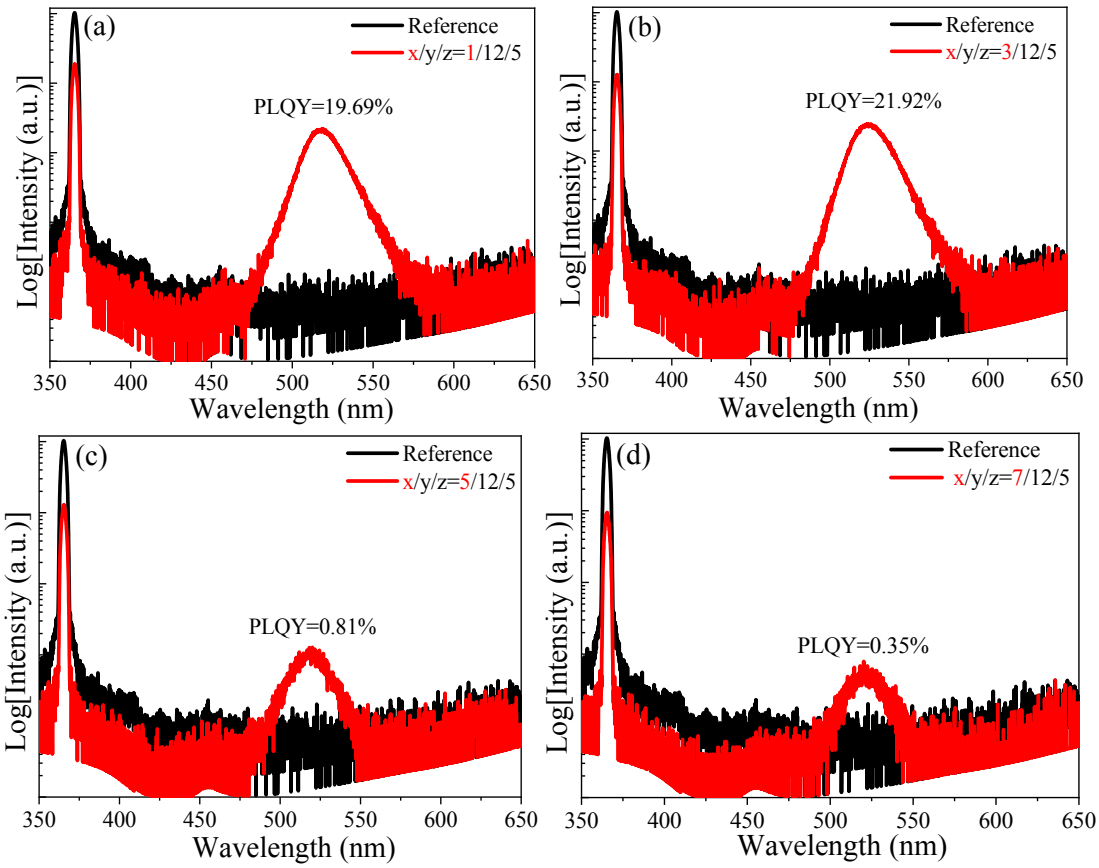

Figure S3. Quantitative PL spectra of dual-phase glasses with fixed 12 mol% CsBr, fixed 5 mol% YbF_3 and different PbO contents: (a) x=1 mol%, (b) x=3 mol%, (c) x=5 mol% and (d) x=7 mol%. PLQY values, defined as the ratio of emitted photons to absorbed photons, can be accordingly calculated. The reference for PLQY measurement is the blank glass without perovskite components, and the sharp peak at 365 nm is the excitation light (the integrated area represents the absorbed intensity).

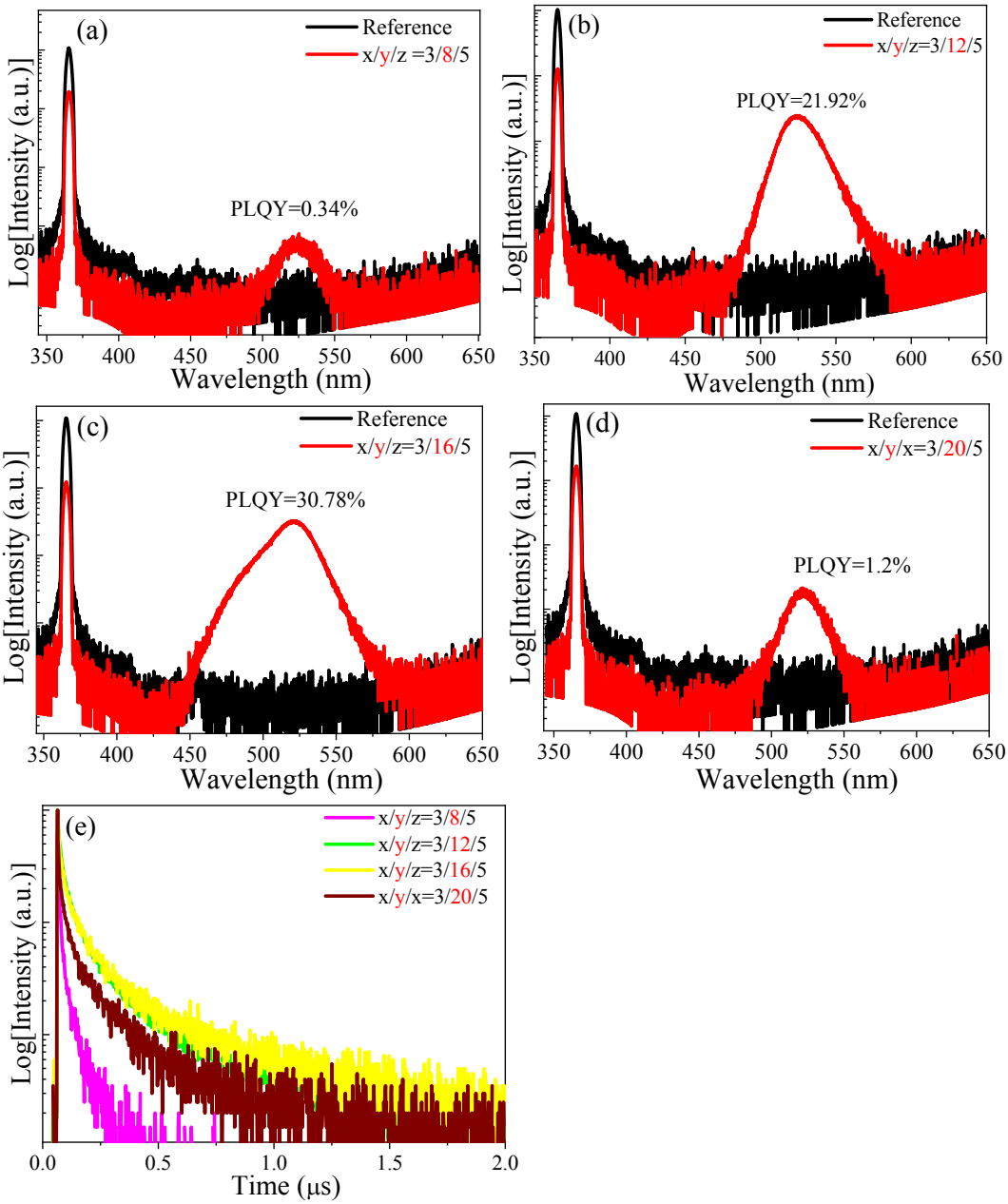

Figure S4. Quantitative PL spectra of dual-phase glasses with fixed 3 mol% PbO, fixed 5 mol% YbF_3 and different CsBr contents: (a) y=8 mol%, (b) x=12 mol%, (c) x=16 mol% and (d) x=20 mol%. PLQY values, defined as the ratio of emitted photons to absorbed photons, can be accordingly calculated. (e) The corresponding PL decay behaviors shows the same variation tendency as PLQYs.

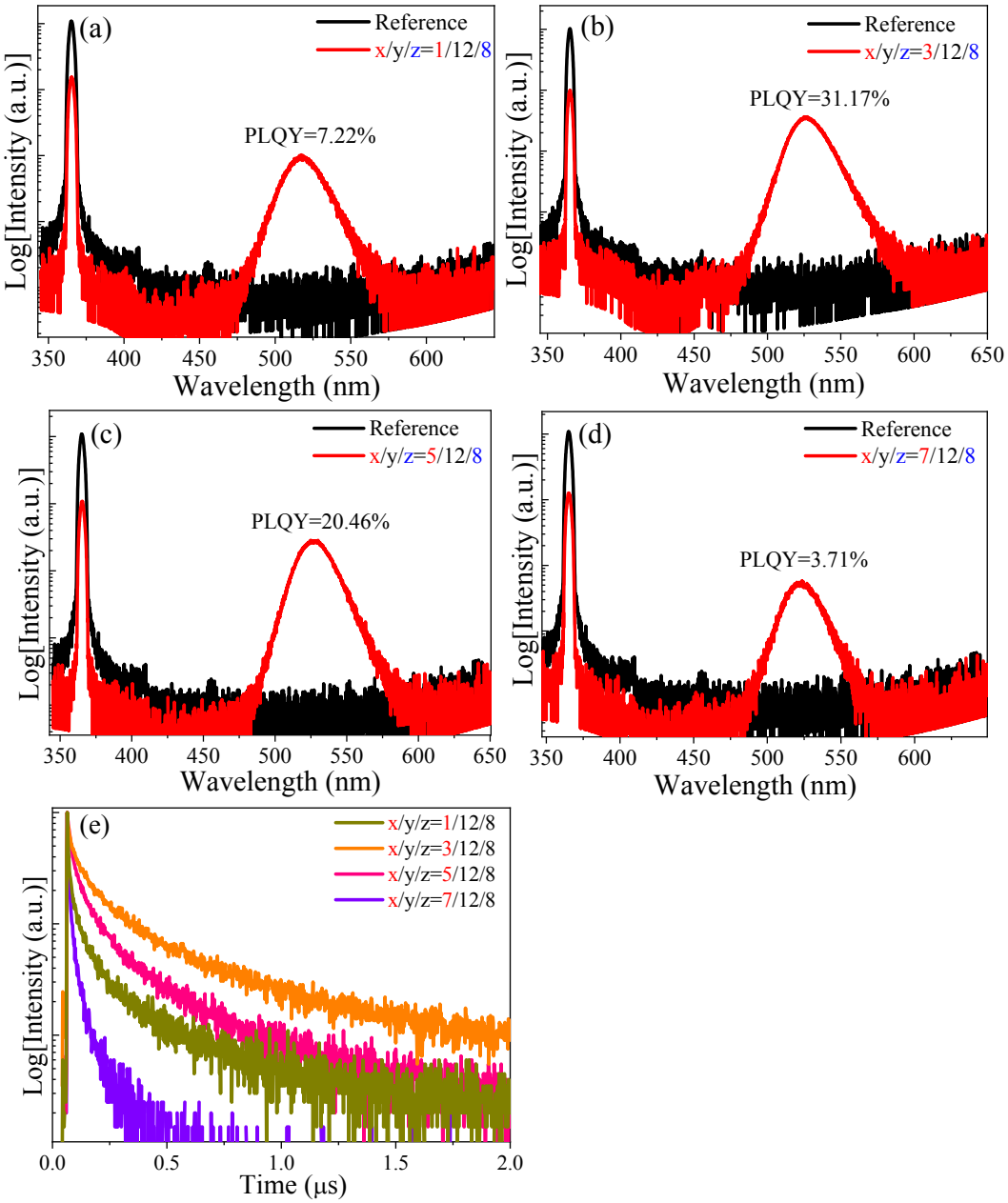

Figure S5. Quantitative PL spectra of dual-phase glasses with fixed 12 mol% CsBr, fixed 8 mol% YbF_3 and different PbO contents: (a) x=1 mol%, (b) x=3 mol%, (c) x=5 mol% and (d) x=7 mol%. PLQY values, defined as the ratio of emitted photons to absorbed photons, can be accordingly calculated. (e) The corresponding PL decay behaviors shows the same variation tendency as PLQYs.

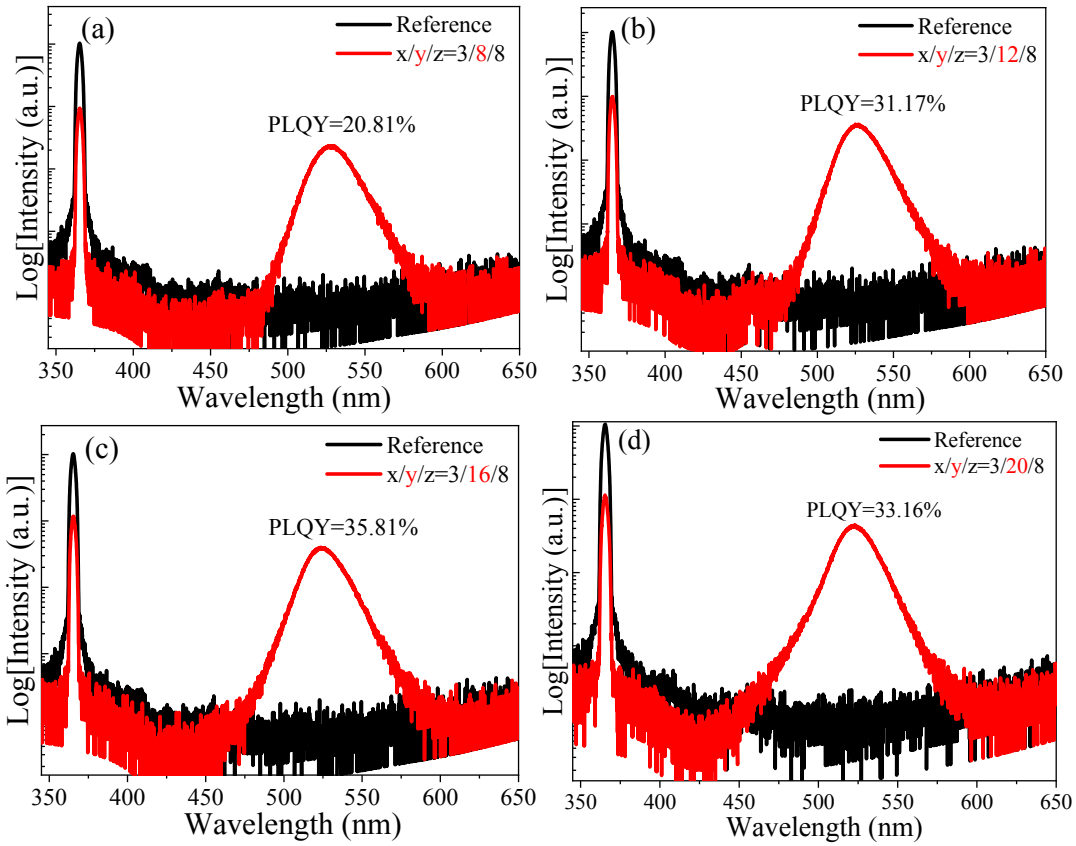

Figure S6. Quantitative PL spectra of dual-phase glasses with fixed 3 mol% PbO, fixed 8 mol% YbF_3 and different CsBr contents: (a) y=8 mol%, (b) x=12 mol%, (c) x=16 mol% and (d) x=20 mol%. PLQY values, defined as the ratio of emitted photons to absorbed photons, can be accordingly calculated.

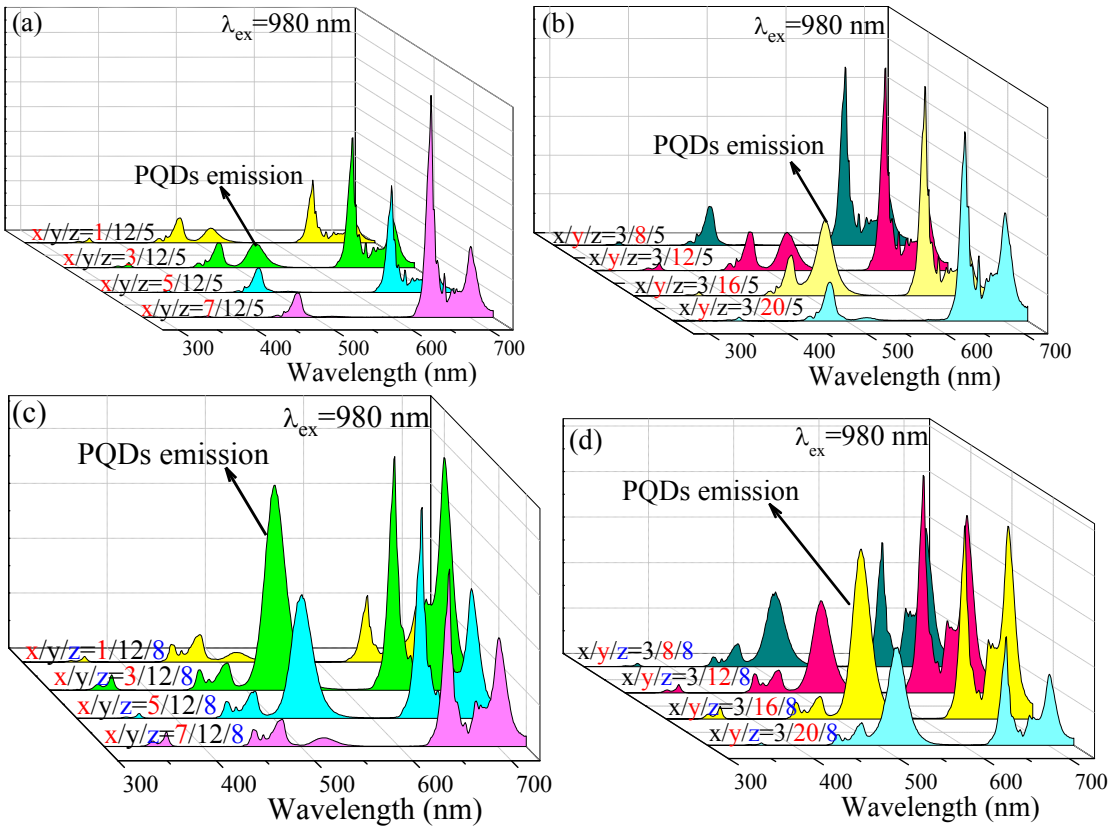

Figure S7. UC emission spectra of a series of dual-phase glasses under the excitation of 980 nm NIR laser: (a) various PbO contents (1~7 mol%, fixed 12 mol% CsBr and 5 mol% YbF_3), (b) various CsBr contents (8~20 mol%, fixed 3 mol% PbO and 5 mol% YbF_3), (c) various PbO contents (1~7 mol%, fixed 12 mol% CsBr and 8 mol% YbF_3) and (d) various CsBr contents (8~20 mol%, fixed 3 mol% PbO and 8 mol% YbF_3). All the samples show typical 523 nm UC emission band originated from exciton recombination of $CsPbBr_3$ PQDs inside the glasses.

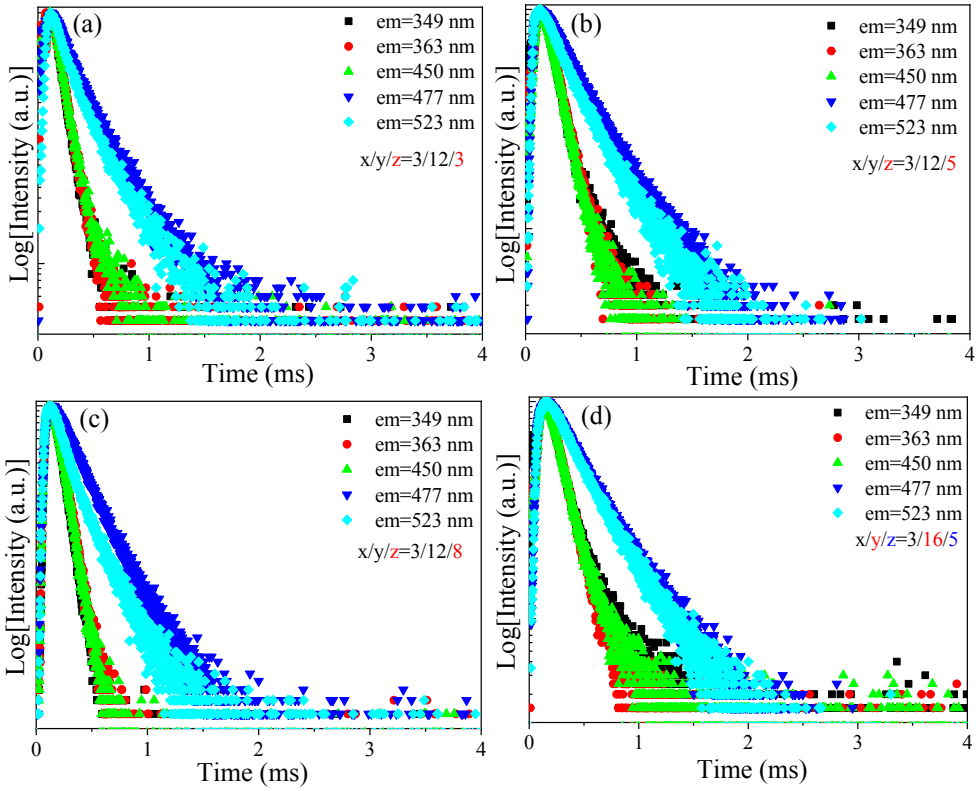

Figure S8. UC decay curves for a series of dual-phase glasses by monitoring 349 nm ($^1I_6 \rightarrow {}^3F_4$), 363 nm ($^1D_2 \rightarrow {}^3H_6$), 450 nm ($^1D_2 \rightarrow {}^3F_4$), 477 nm ($^1G_4 \rightarrow {}^3H_6$) emissions of Tm^{3+} and 523 nm exciton recombination of $CsPbBr_3$ PQDs: (a-c) different contents of YbF_3 component (3, 5, 8 mol%) in glasses with fixed 3 mol% PbO and 12 mol% CsBr, and (d) 3 mol% PbO, 16 mol% CsBr and 5 mol% YbF_3 components in the glass.

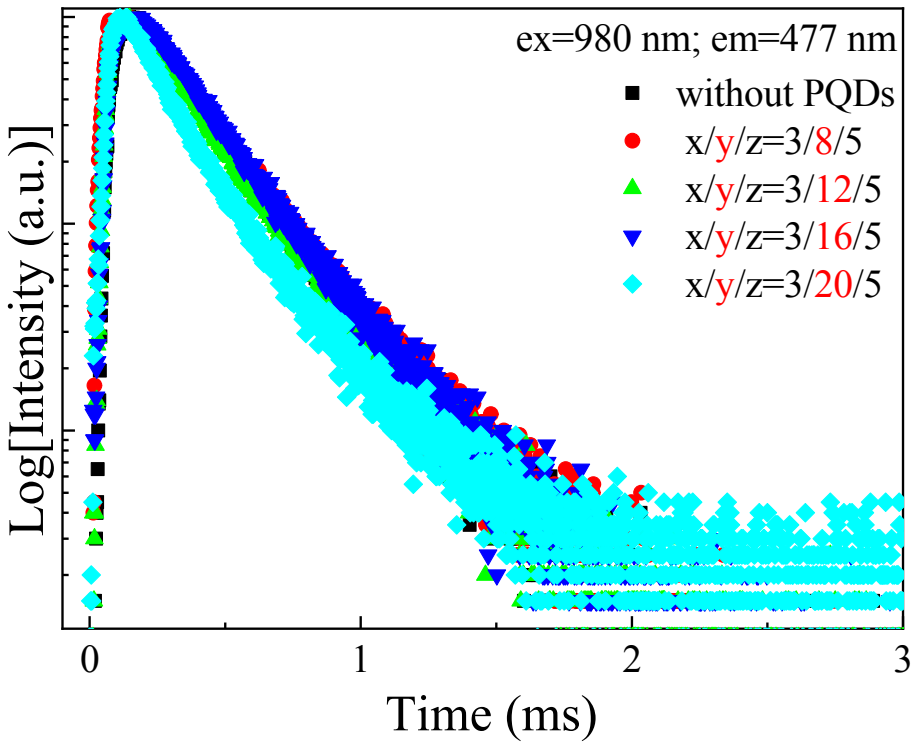

Figure S9. UC decay curves for a series of dual-phase glasses with different contents of CsBr component (8~20 mol%, fixed 3 mol% PbO and 5 mol% YbF_3) by monitoring Tm^{3+} 477 nm ($^1G_4 \rightarrow {}^3H_6$) emission. As a comparison, UC decay of Tm^{3+} $^1G_4$ emitting state for the glass containing only Tm: NaYbF4 NCs (without $CsPbBr_3$ PQDs) is provided. Evidently, decay behaviors of Tm^{3+} $^1G_4$ emitting state are almost identical for all the samples.

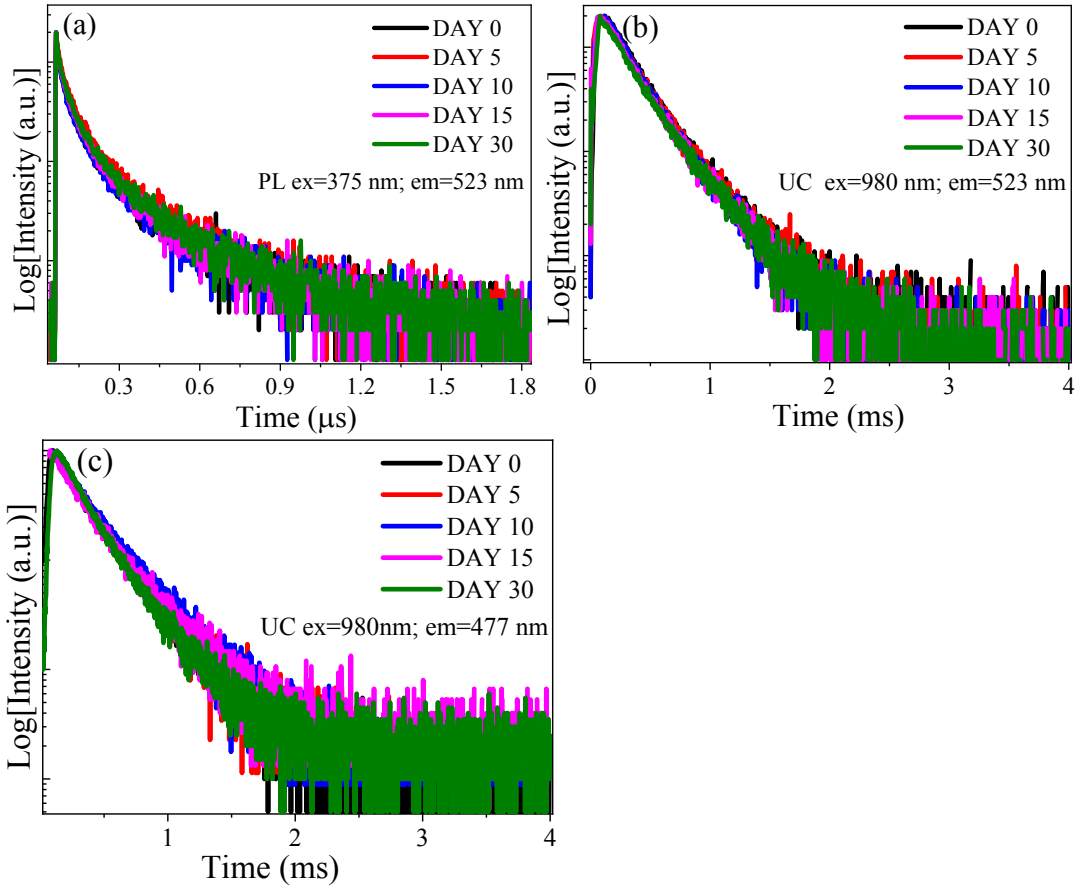

Figure S10. Long-term stability test by directly immersing dual-phase glass in water for 30 days and recording (a) PL decays of exciton recombination, (b) UC decays of exciton recombination and (c) UC decay of Tm^{3+} 477 nm ($^1G_4 \rightarrow {}^3H_6$) emission. With elongation of storing time in water, PL decay of exciton recombination and UC radiative kinetics of exciton recombination and Tm^{3+} $^1G_4 \rightarrow {}^3H_6$ transition in the dual-phase glass are not remarkably altered.

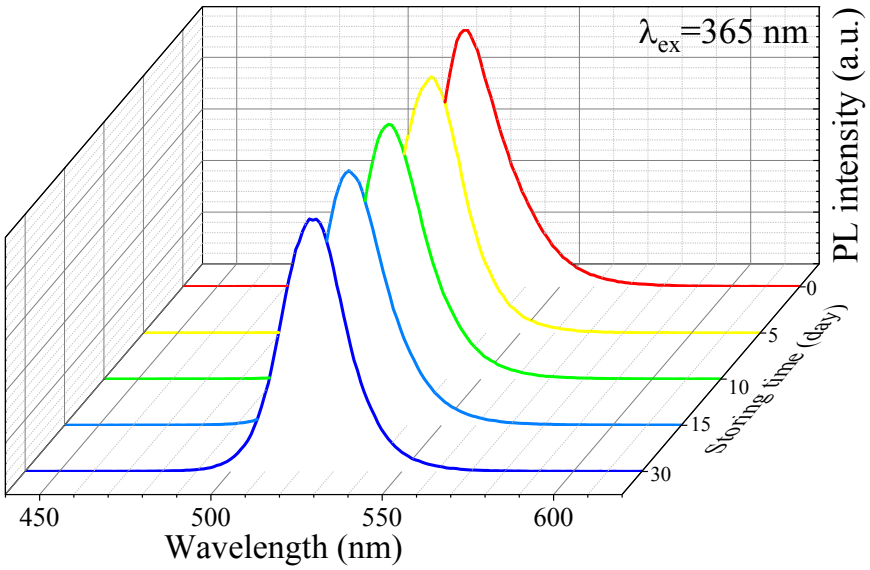

Figure S11. Long-term stability test by directly immersing dual-phase glass in water for 30 days and recording the corresponding PL spectra of exciton recombination. With increase of immersing time from 0 to 30 days, no obvious change in PL intensity and spectral profile.

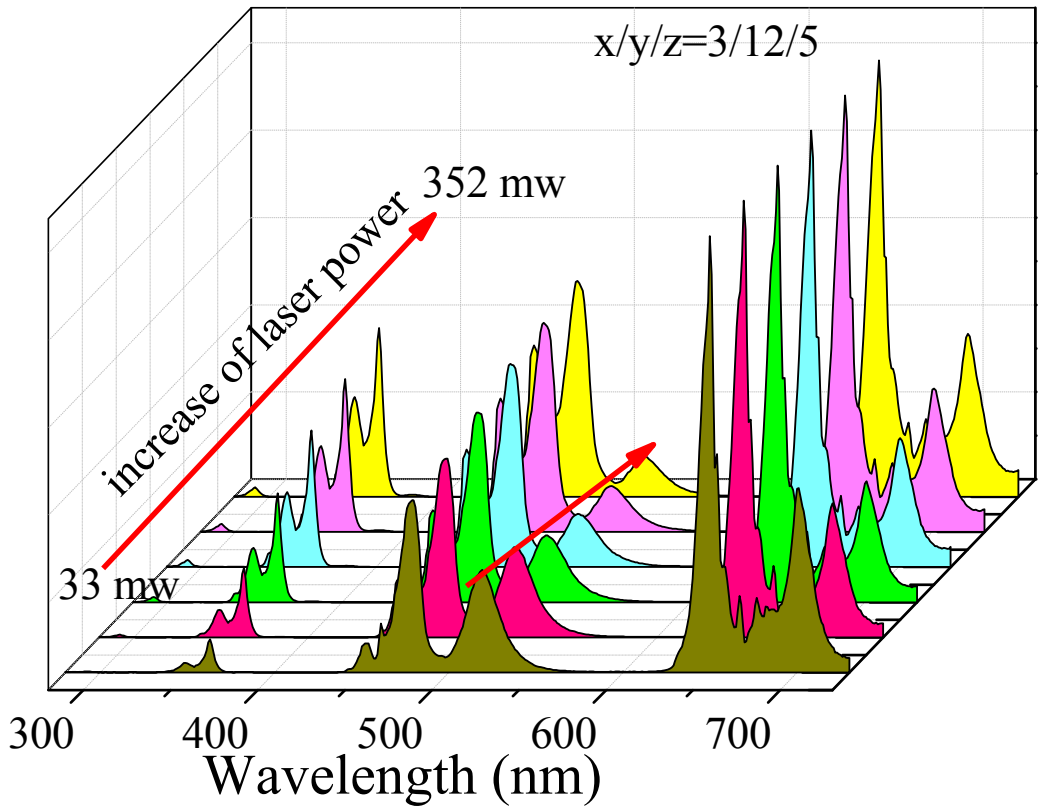

Figure S12. UC emission spectra for Tm: $NaYbF_4$ & $CsPbBr_3$ dual-phase glass under single-modal excitation at 980 nm with different laser power. All the spectra are normalized to Tm^{3+} 477 nm ($^1G_4 \rightarrow {}^3H_6$) emission. With increase of NIR laser power, 523 nm UC emission intensity from exciton recombination gradually weakens owing to laser-induced thermal quenching of exciton recombination.

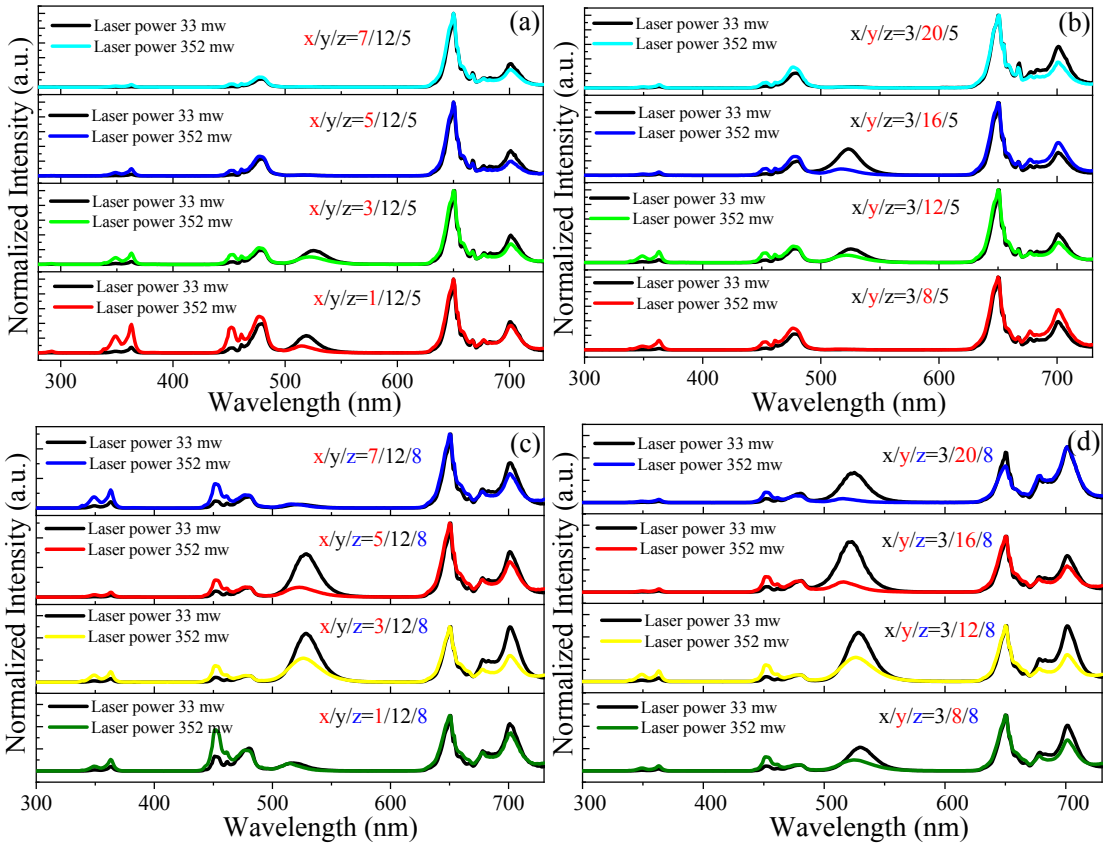

Figure S13. Normalized UC emission spectra for a series of dual-phase glasses under single-modal excitation at 980 nm with low/high (33 mW or 352 mW) laser power: (a) various PbO contents (1~7 mol%, fixed 12 mol% CsBr and 5 mol% YbF_3), (b) various CsBr contents (8~20 mol%, fixed 3 mol% PbO and 5 mol% YbF_3), (c) various PbO contents (1~7 mol%, fixed 12 mol% CsBr and 8 mol% YbF_3) and (d) various CsBr contents (8~20 mol%, fixed 3 mol% PbO and 8 mol% YbF_3). Compared to the case of low-power laser excitation, 523 nm UC emission intensity from exciton recombination weakens upon high-power laser excitation for all the samples.

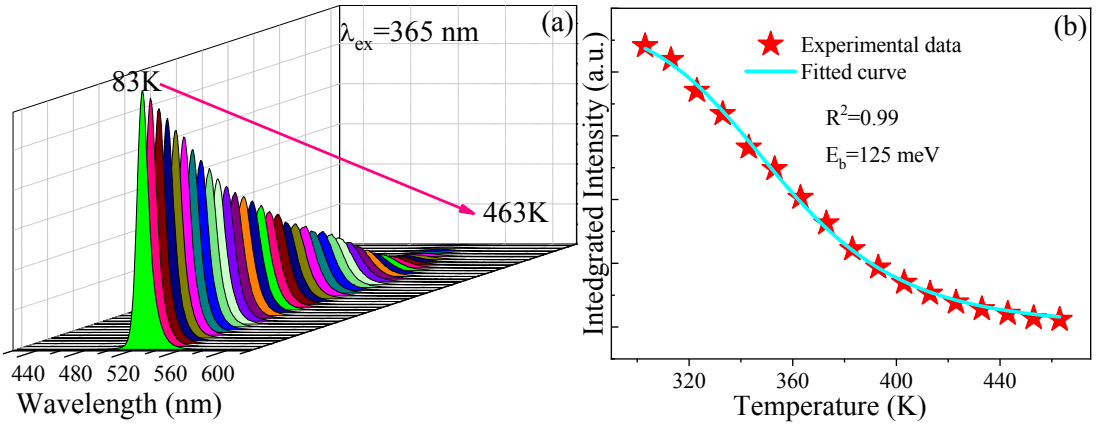

Figure S14. (a) Temperature-dependent PL spectra of dual-phase glass under 365 nm UV light excitation. (b) Integrated emission intensity of $CsPbBr_3$ PQDs as a function of temperature. The fitted curve and the obtained exciton recombination energy (E_b) are provided in the figure.

The important physical parameter of exciton binding energy of $CsPbBr_3$ PQDs inside glass can be estimated with the following equation [7,25]

$$I(T) = \frac{I_0}{1 + Aexp^{-E_{b/(k_BT)}}}$$

where $I(T)$ and I_0 are PL intensities at temperature T and 0 K, respectively, T is absolute temperature, A is a pre-exponential constant, k_B is Boltzmann constant and E_b is exciton binding energy. With increase of temperature, the integrated emission intensity of $CsPbBr_3$ PQDs rapidly decreases, which is caused by temperature quenching. The exciton binding energy is 125 meV by fitting the experimental data with the above-mentioned expression.

*References 7 and 25 are listed in the manuscript.

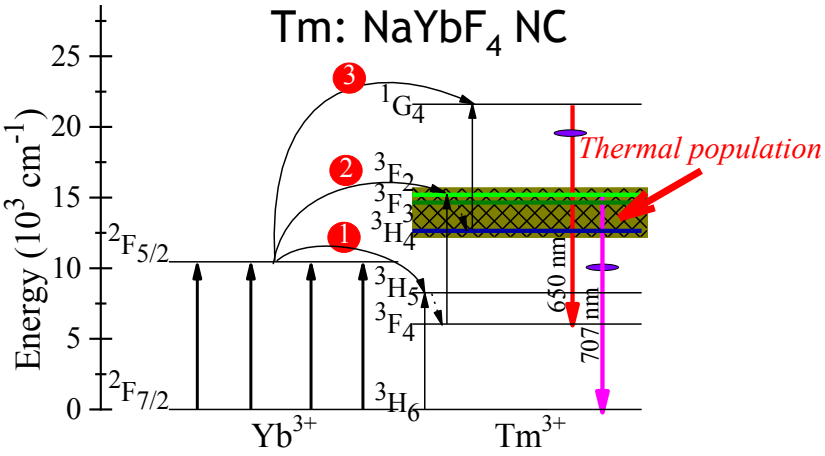

Figure S15. Energy level diagrams of Yb^{3+} and Tm^{3+} ions, showing the thermally coupled states of $^3H_4$ and $^3F_{2,3}$ and the possible energy transfer processes to populate $^3H_4$, $^3F_{2,3}$ and $^1G_4$ emitting-states of Tm^{3+}.

The $^3F_{2,3}$ and $^3H_4$ states of Tm^{3+} are eligible to act as thermally coupled states because of the suitable energy gap between them (~ 2000 cm^{-1}). With increase of temperature, the $^3F_{2,3}$ states are populated via thermal activation while the $^3H_4$ state is depopulated. The population of $^1G_4$ state of Tm^{3+} is originated from $^3H_4$ one. Therefore, temperature sensitive fluorescence intensity ratio (FIR) of Tm^{3+} between $^3F_{2,3} \rightarrow {}^3H_6$ transition (707 nm) and $^1G_4 \rightarrow {}^3F_4$ one (650 nm) is expected.